Kondo effect and spin-glass behavior of dilute iron clusters in silver films

W. T. Herrera,[1,*] Y. T. Xing,[1] S. M. Ramos,[1] P. Munayco,[1] M. B. Fontes,[1] E. M. Baggio-Saitovitch,[1] and F. J. Litterst[2]

[1]*Centro Brasileiro de Pesquisas Físicas, Rua Dr. Xavier Sigaud 150, 22290-180, Rio de Janeiro, Brazil*

[2]*Institute for Physics of Condensed Matter, Technische Universität Braunschweig, Mendelssohnstrasse 3, D-38106 Braunschweig, Germany*

(Received 30 June 2009; revised manuscript received 16 May 2011; published 28 July 2011)

Thin films of silver containing 0.3–1.5% Fe have been prepared by vapor codeposition. Depending on substrate temperature and iron concentration, we could systematically follow the formation of nanometer-size clusters of iron from initially dilute iron monomers. Samples were characterized via x-ray diffraction, resistivity, magnetization, susceptibility, and Mössbauer spectroscopic measurements. For samples with iron concentrations below 1% prepared at low temperatures, we find clear evidence for the Kondo effect. For higher concentrations, all studied samples reveal a nonmonotonic variation of resistivity with temperature, which can be understood by competing shielding of the cluster moments by conduction electron-spin scattering due to the Kondo effect and the magnetic coupling. The magnetic behavior can be best described with an ensemble of ferromagnetic particles. The magnetic freezing observed at low temperatures is assumed to be mainly controlled via the interparticle interactions mediated via conduction electron polarization, i.e., a Ruderman-Kittel-Kasuya-Yosida interaction.

DOI: 10.1103/PhysRevB.84.014430 PACS number(s): 75.75.−c, 72.15.Qm, 75.50.Lk, 76.80.+y

I. INTRODUCTION

Dilute magnetic impurities in nonmagnetic metallic matrices have been intensively studied in the past to investigate the single-ion Kondo effect in the parts-per-million concentration range and the development of spin-glassy behavior upon increasing magnetic interactions with doping below several 1000 ppm. Concentrated Kondo lattice systems have become an essential constituent for a new understanding of phenomena relating magnetism and superconductivity in solids. Most recently, there is increasing interest in dilute systems with magnetic nanoclusters in the 1–10 nm range in a nonmagnetic surrounding, which is mainly related to the electronic properties of quantum dots. Systems ranging between the very dilute Kondo impurity regime and magnetic nanoclusters have been less studied.

We therefore have started an investigation of iron nanoclusters formed in nonmagnetic hosts with low solubility. These are very dilute clusters possessing high magnetic moments, however, with weak magnetic intercluster interactions, and one may expect a competition between the Kondo effect and magnetic coupling. The magnetic interaction is expected to originate mainly from the Ruderman-Kittel-Kasuya-Yosida (RKKY) mechanism via conduction electron polarization.

Fe precipitates in metals can be studied following various tracks of preparation. Mostly precipitates are formed from concentrated solid solutions by thermal treatment. A less common approach is starting out from very dilute Fe impurities embedded in the metal host and subsequent annealing leading to diffusion of impurities and clustering. For characterizing the electronic state of Fe in these precipitates and its magnetic properties, Mössbauer spectroscopy is a highly suitable method. One system of interest with very low miscibility in the solid and liquid state is Ag:Fe. Even very dilute alloys with a low concentration of Fe in Ag may only be achieved via nonequilibrium preparation, i.e., vapor deposition,[1,2] electron-beam coevaporation,[3] mechanical alloying,[4] or implantation.[5,6] Well known are the early Mössbauer spectroscopic studies of ppm concentrations of Fe in Ag prepared via diffusion of ^{57}Co into the host matrix with the radioactive decay of ^{57}Co leading to ^{57}Fe (see Ref. 7). Morales *et al.*[1] succeeded in preparing films in the range of percent concentration of Fe in Ag by evaporating the elements in proper proportion and codepositing them onto Kapton substrates kept at 16 K. From the Mössbauer spectra, isolated monomeric and dimeric Fe in the Ag matrix were identified as major components. In addition, a minor contribution was found which was attributed to clusters of fcc iron. Upon annealing at room temperature, the formation of clusters was enhanced, but only for annealing around 480 K, bcc Fe precipitates were formed. The various species were identified from their different hyperfine parameters.

II. EXPERIMENT

In continuation of these studies, we prepared films by codeposition of Fe and Ag with nominal concentrations between 0.3% and 1.5% of Fe. We have characterized the samples by x-ray diffraction, ^{57}Fe Mössbauer spectroscopy, magnetization, susceptibility, and electrical resistivity measurements. In order to achieve a sufficient amount of ^{57}Fe to perform Mössbauer experiments, we used iron metal enriched to 90% in ^{57}Fe. The preparation procedure and the evaporation facility were the same as described in Refs. 1,2, and 8. The base vacuum pressure in the deposition chamber was 2×10^{-9} mbar, increasing to 2×10^{-8} mbar during deposition. The films were deposited onto Kapton foils kept either at 285 or 85 K. The deposition rate was monitored using piezocrystals and typical values were 4 Å/s for Ag and 0.02 Å/s for Fe (see Table I). The total film thicknesses were typically 1 to 4 μm. Nominal thicknesses and concentrations were confirmed by *energy dispersive x-ray spectroscopy* in experiments of the same installation for various concentrations of iron. Under these preparation conditions, we expected clusters to be formed directly during the deposition process and not only after annealing.

The first sets of Mössbauer experiments were performed *in situ*, i.e., in the cryostat where the preparation was done. The spectrometer was of a standard type with sinusoidal velocity sweep. The ^{57}CoRh source was kept at room temperature. It

TABLE I. η deposition rates, T_s substrate temperature, t deposition time, and ξ thickness.

% Fe	η_{Fe} (Å/s)	η_{Ag} (Å/s)	T_s(K)	t (min)	ξ (μm)
0.3	0.009	4.0	285	120	2.8(3)
0.5	0.01	3.0	285	115	2.7(3)
0.8	0.007	1.3	285	124	1.0(2)
1.0	0.028	4.05	285	117	2.8(3)
1.2	0.031	1.55	285	120	1.1(2)
1.5	0.035	4.6	285	130	3.6(3)
1.0	0.02	4.5	85	124	3.3(3)
0.4	0.01	3.9	85	140	3.3(3)
0.0	0.0	3.0	285	140	2.3(3)

turned out that the films could be transferred to a variable temperature cryostat (1.5–300 K) without observing any change of the spectra. So it was possible to perform *ex situ* experiments without inducing structural changes of the films. Spectra were also taken in various applied magnetic fields up to 7T at various temperatures. Magnetization and ac susceptibility were measured in a superconducting quantum interference device (SQUID) magnetometer [magnetic property measurement system (MPMS) model of quantum design].

Resistivity measurements were performed between 1.5 and 300 K using a standard four-contacts technique with an ac LR720 multiplexer bridge (Linear Research). Magnetoresistance was measured with fields up to 7.5T applied perpendicular to the film plane. X-ray diffraction was performed on a Rigaku MiniFlex using Cu $K_{\alpha 1}$ and $K_{\alpha 2}$.

III. RESULTS AND DISCUSSION

X-ray diffraction of the iron-doped films revealed significant broadenings of the silver Bragg peaks, indicating the formation of small grains. Using the Scherrer formula, we estimate mean grain sizes of about 22 and 11 nm for films deposited onto 285 and 85 K substrates, respectively. All films reveal a high degree of texture (see Fig. 1).

Figure 2 (left side) shows a series of Mössbauer spectra taken at 300 K for various concentrations of iron in films prepared at 285 K. Below 1% Fe, the spectra are composed of a superposition of three subspectra. One singlet line S can be identified as being caused by iron monomers;[1,5,9,10] in addition, we observed two quadrupole split doublets, which for all concentrations have practically the same hyperfine parameters. For comparison with the previous results by Morales *et al.*,[1] we undertook a reanalysis of those data. It turned out that they can in fact be better fitted using the monomer signal and the two doublet contributions found in the analysis of our new samples.

We label these two doublets as DI and DII. The hyperfine parameters and the variation of their relative intensities for the three species are shown in Fig. 3. The relative amount of monomers is continuously decreasing with increasing iron concentration, and, finally, for more than 1% Fe, the singlet subspectrum can no longer be traced and only a superposition of the two quadrupole doublets is found (left side of Fig. 2).

Whereas the relative spectral area of DI is decreasing with increasing iron concentration, the area of DII is increasing. A close-lying possible interpretation for the two doublets would

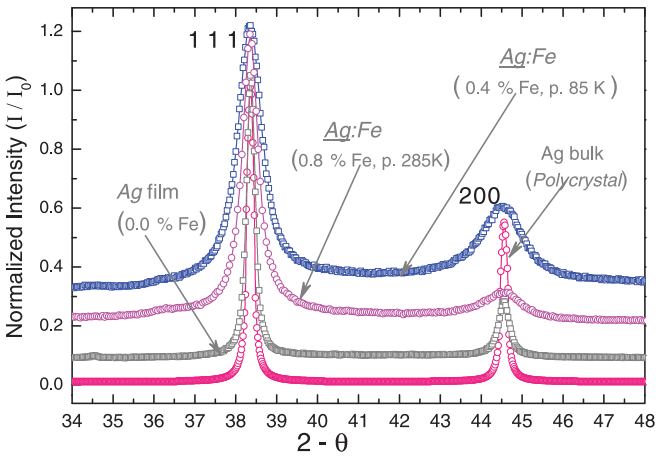

FIG. 1. (Color online) X-ray diffraction of polycrystalline Ag, a pure Ag film, and iron-doped Ag films deposited onto 285 and 85 K substrates.

be to attribute them to iron on the surface and from the core of one single type of cluster. From the variation of relative areas with concentration, one then would have to relate DI to the surface and DII to the core which, however, would imply cluster sizes in the micrometer range. This definitely can be excluded since such clusters should have an fcc or bcc structure and reveal magnetic blocking in the 100 K range or even higher, which is not observed (see below).

We attribute the doublets to two distinctly different kinds of clusters in the nanometer range, with DI representing clusters of smaller size and DII representing clusters of bigger size. DI has the higher isomer shift rather close to the value of

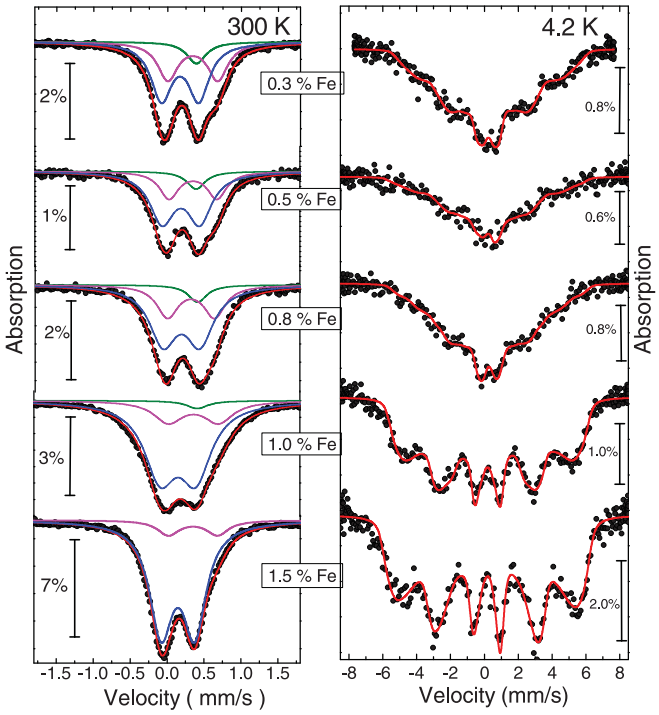

FIG. 2. (Color online) Comparison of Mössbauer spectra of iron silver films prepared at 285 K with 0.3, 0.5, 0.8, 1.0, and 1.5% Fe, taken at 300 K (left) and 4.2 K (right). Values of absorption are indicated by bars near the individual spectra.

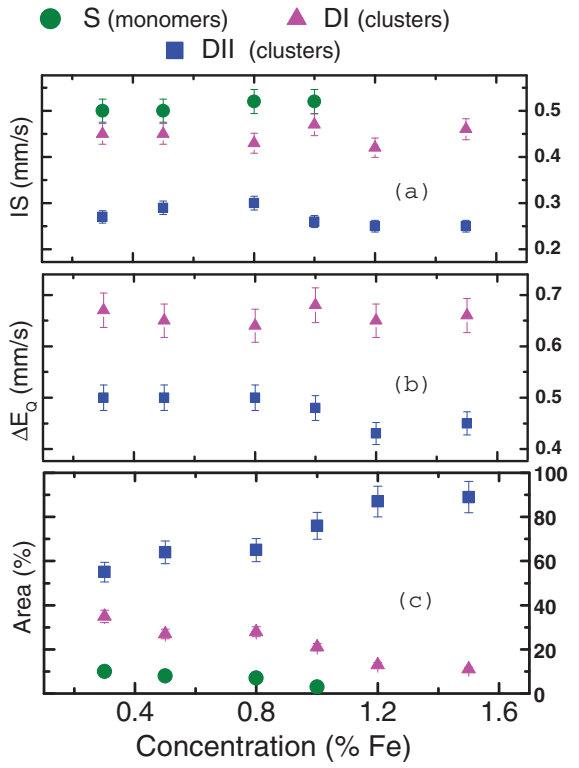

FIG. 3. (Color online) Hyperfine parameters for iron silver films prepared at 285 K: (a) isomer shift IS vs iron metal at 300 K, (b) quadrupole splitting ΔE_Q, and (c) relative spectral areas of the subspectra S (monomers), DI, and DII (clusters).

the monomer and a larger quadrupole splitting indicative of a low-symmetry surrounding. The isomer shift for DII is smaller, meaning that the number of iron neighbors is higher; the quadrupole splitting is smaller, i.e., coming closer to a cubic arrangement.

From these experimental data alone, however, the shape of clusters cannot be derived. Calculations of the hyperfine parameters for possible cluster configurations embedded into the silver matrix are needed, which also will allow a comparison with the stable free iron cluster studied by Rollman *et al.*[11] Due to the formation of clusters, their effective concentration is reduced against the nominal iron concentration. Consequently, we are still dealing with a reasonably dilute system, yet consisting of big moments that are assumed to be interacting via RKKY coupling.

For temperatures below 15 K, we find an onset of magnetic hyperfine interaction connected with the freezing of the cluster magnetic moments for all the studied films. The Mössbauer spectra taken at 4.2 K are shown in Fig. 2 (right side). It is clearly seen that there is a distribution of the magnetic hyperfine interaction, which becomes better defined with an increasing iron concentration, i.e., with a larger number of clusters. The drawn lines through the data points of the spectra are simplistic fits using a distribution of hyperfine fields. For the present discussion, it may suffice to notice the onset of the magnetic interaction. A more detailed interpretation of these patterns, taking into account the role played by magnetic fluctuations, cluster-cluster interactions, etc., will be presented elsewhere.

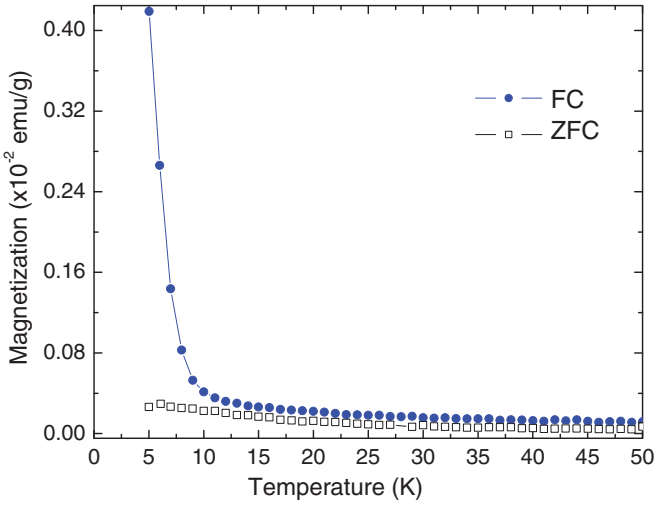

FIG. 4. (Color online) Temperature dependence of dc magnetization for an iron silver film with 1% Fe prepared at 285 K.

In the same temperature range where the magnetic hyperfine spectra indicate freezing of spin fluctuations, magnetization data reveal a clear irreversibility between zero field and applied field cooling (see, e.g., Fig. 4 for 1% Fe). Further evidence for spin freezing comes from ac susceptibility (100 Hz), which displays a cusp close to the same temperature where dc magnetization reveals the onset of irreversibilities (Fig. 5). The close-lying freezing temperatures, derived from magnetic hyperfine interaction, susceptibility, and magnetization with their very different characteristic time windows, indicate a considerable intercluster interaction. In contrast, noninteracting clusters should result in distinctly different freezing behavior for the various methods due to their differing time scales.

We also have performed Mössbauer measurements in an applied magnetic field over a wide temperature range above freezing. The spectra were analyzed with a distribution of magnetic hyperfine fields (see Fig. 6) assuming a full polarization of the moments along the applied field. We are

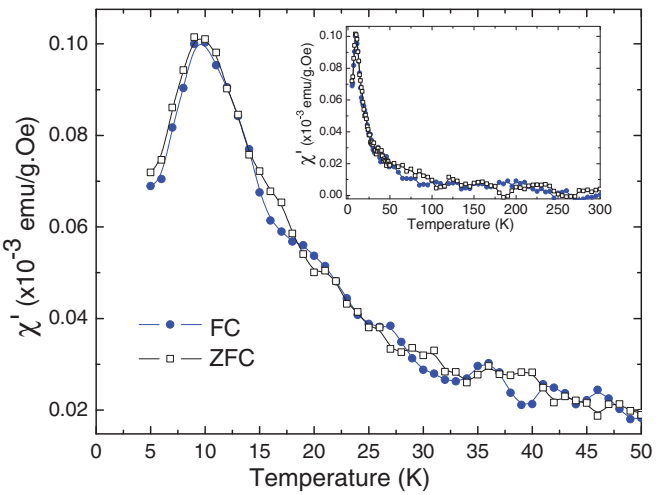

FIG. 5. (Color online) Temperature dependence of ac (100 Hz) susceptibility for an iron silver film with 1% Fe prepared at 285 K. Mass refers to silver.

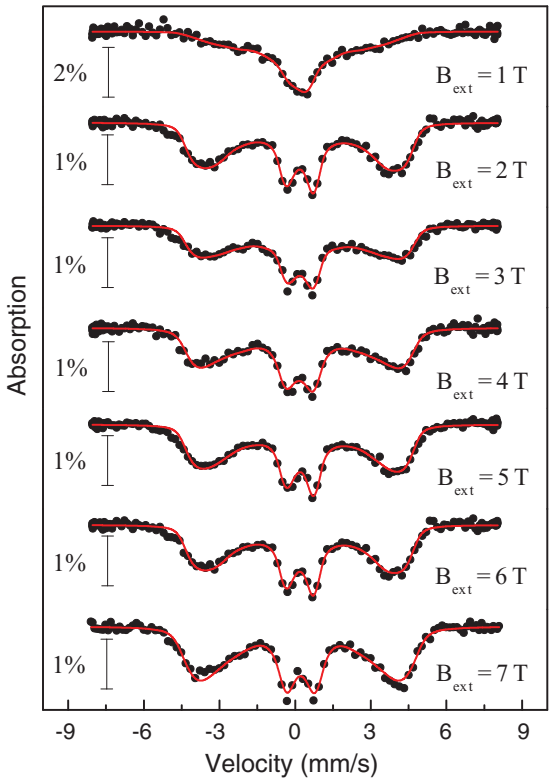

FIG. 6. (Color online) Mössbauer spectra of iron silver films with 1% Fe prepared at 285 K, taken at 30 K, with different external magnetic fields applied.

able to describe the applied field and temperature dependence of the mean magnetic hyperfine splitting with a modified Brillouin function[12] (see Fig. 7) with an effective spin 1/2, which is appropriate for particles with uniaxial magnetic anisotropy having only up or down orientation. The fit yields an average magnetic moment of 35(2)μ_B, giving evidence that the components DI and DII are indeed related to small ferromagnetic clusters. Fits using a Langevin function

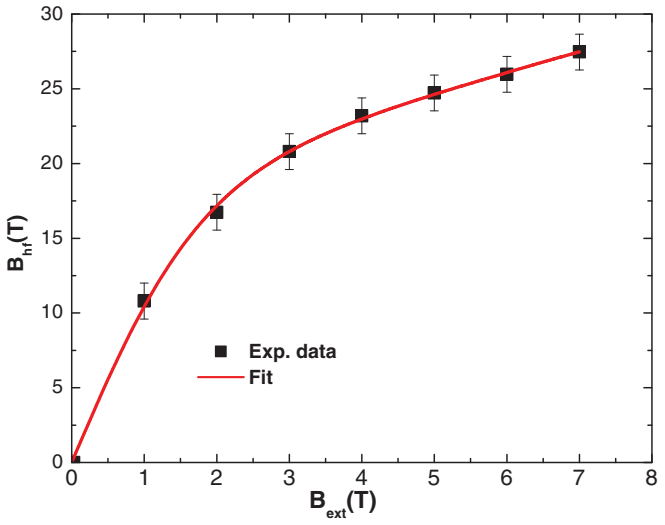

FIG. 7. (Color online) Plot of mean hyperfine fields vs external applied field for an iron silver film with 1% Fe prepared at 285 K, taken at 30 K, and fit with an effective spin-1/2 Brillouin function.

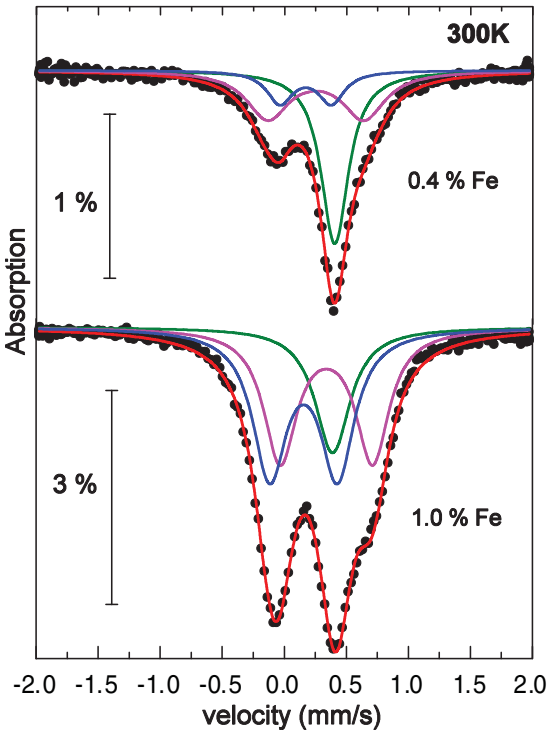

FIG. 8. (Color online) Mössbauer spectra taken at 300 K for iron silver samples with 0.4% and 1.0% Fe (samples prepared at 85 K). Singlet line: monomer; doublets: clusters DI and DII.

give similar values for the moment. From bulk and local magnetization (as derived from the Mössbauer data) above the spin freezing temperature, it is not possible to decide whether an analysis assuming uniaxial anisotropy or rather an isotropic model is more appropriate. The origin for uniaxial anisotropy could be related to the very small size of clusters with possibly nonspherical shape. The extrapolated saturation mean hyperfine field is about 31(1)T, which in a metallic system corresponds to about 2–2.5 μ_B. The temperature dependence of ac susceptibility follows a Curie-Weiss behavior with moments of 40(2) μ_B, which is in good agreement with the Mössbauer data taken in an applied field.

The room-temperature Mössbauer spectra of the samples prepared at 85 K reveal the same three species, S, DI, and DII, yet with a clearly higher contribution by the monomer S (see Fig. 8). At 4.2 K, the sample with 1.0% Fe shows a magnetic hyperfine pattern (right side of Fig. 9), which, however, indicates a lower degree of freezing than found for the sample prepared at 285 K (see right side of Fig. 2). For the sample with 0.4% Fe, there is still no indication of a magnetic hyperfine interaction at 4.2 K (Fig. 8).

When comparing the freezing behavior, one has to take into account that the concentration of clusters in the samples prepared at 285 K (with dominant contribution from the bigger clusters of type DII) is in fact lower than in the samples prepared at 85 K, so their distances are larger than those between the isolated monomers for the same nominal concentration of iron. Their interaction, however, is increased due to the augmented moment of each cluster and one can thus understand the stronger tendency for freezing with increasing concentration despite longer distances between clusters. Using

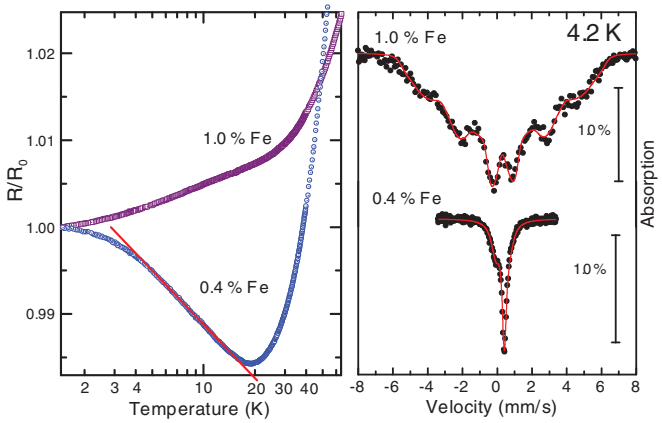

FIG. 9. (Color online) Left: electrical resistivity for iron silver samples with 0.4% and 1.0% Fe prepared at 85 K, normalized to R_0 ($T = 1.5$ K); right: spectra taken at 4.2 K of the same samples.

a RKKY model adopted for clusters[13] with the known Fermi surface vectors of silver and ferromagnetic cluster moments with about 40 μ_B, we arrive for our concentrations at average cluster-cluster interaction energies corresponding to 10–20 K, in agreement with the freezing temperatures derived from the Mössbauer, susceptibility, and magnetization data.

Resistivity results for samples prepared at 85 and 285 K are shown in Fig. 9 (left) and Fig. 10, respectively. For low iron concentrations of the 285 K preparations, we find clear minima in the temperature dependence of the resistivity (typically around 20 K) followed by maxima at lower temperatures. The minima are indicative for the onset of the Kondo effect. The typical logarithmic increase of resistivity with decreasing temperature may most clearly be traced for the samples with low concentrations prepared at 85 K, i.e., containing

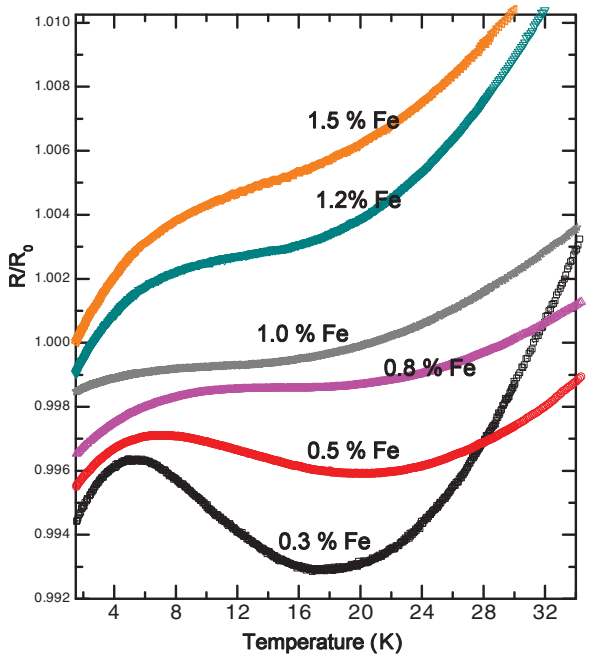

FIG. 10. (Color online) Electrical resistivity for iron silver samples with 0.3, 0.5, 0.8, 1.0, 1.2, and 1.5% Fe prepared at 285 K, normalized to R_0 ($T = 1.5$ K), but shifted for better visibility.

a high number of monomers (see Fig. 9). Our resistivity measurements in applied magnetic fields reveal the expected suppression of the Kondo effect and a turnover to the magnetic state (see Fig. 11). Saturation of resistivity without an applied field is only achieved below about 2 K, which is in agreement with earlier data obtained by Mössbauer,[7] time-differential perturbed angular correlation (TDPAC),[14,15] and susceptibility[16] measurements on Fe monomers in bulk silver where Kondo temperatures of about 1.5–2.0 K were found.

Actually an increased value was derived from the TDPAC[17] for dilute iron impurities in nanocrystalline silver. This discrepancy of T_K found between bulk and nanocrystalline silver was attributed to a pressure-induced increased hybridization of iron 3*d* electrons with the conduction electrons near the grain surfaces.[18,19] Their silver grain size of 19 nm is actually nearly the same as that found for our samples prepared at 285 K with grain sizes of about 22 nm, however, our data do not support an increase of the Kondo temperature.

The Kondo anomaly is known to be strongly controlled by finite-size effects and changing dimensionality as demonstrated, e.g., for Cu:Cr (Ref. 20) and Au:Fe (Ref. 21) films. In fact our film thicknesses are on the order of the dimension of the Kondo cloud, as estimated from the bulk Kondo temperature and the Fermi velocity of silver. Unfortunately our present data are yet not systematic enough to provide evidence for the influence of film thickness.

Resistivity maxima (Fig. 10) are observed for samples containing a higher amount of clusters and also revealing spin freezing from the Mössbauer effect. The decrease of resistivity for temperatures below the maxima is related to the suppression of the Kondo effect by the magnetic interactions. It becomes more pronounced with an increasing concentration of iron, and also with the number of clusters. The shapes of the resistivity curves are in very good qualitative agreement with the calculations of Larsen[22] and, more recently, Vavilov *et al.*,[23] predicting a nonmonotonic variation of resistivity with temperature for concentrated systems in which the RKKY interaction between magnetic impurities is strong compared to the Kondo interaction. Similar observations have been reported, e.g., for Au and Cu matrices doped with Mn and Fe impurities in the 0.1% concentration range.[24] For concentrations above about 1% Fe, the resistivity minimum can no longer clearly be traced in our data and only the turndown of resistivity due to the magnetic freezing is visible. Notably, the resistivity minimum is wiped out for all samples revealing spin freezing from the Mössbauer effect (see Fig. 10).

In Fig. 11 we show the field dependence of resistivity for iron silver samples with 0.4% Fe prepared at 85 K (Fig. 11, left), and with 0.3% Fe prepared at 285 K (Fig. 11, right). It is apparent that the Kondo minimum can be suppressed by smaller fields for the sample prepared at 285 K containing a higher amount of clusters.

Despite being aware that the temperature where the maximum of resistivity occurs does not directly correspond to the spin-glass temperatures as derived, e.g., from the susceptibility cusp (see discussions in Refs. 22 and 24), we plot this temperature T_{on} in Fig. 12 to demonstrate the concentration dependence of spin freezing. The values were obtained from the zero of the first temperature derivative of resistivity for 0.3,

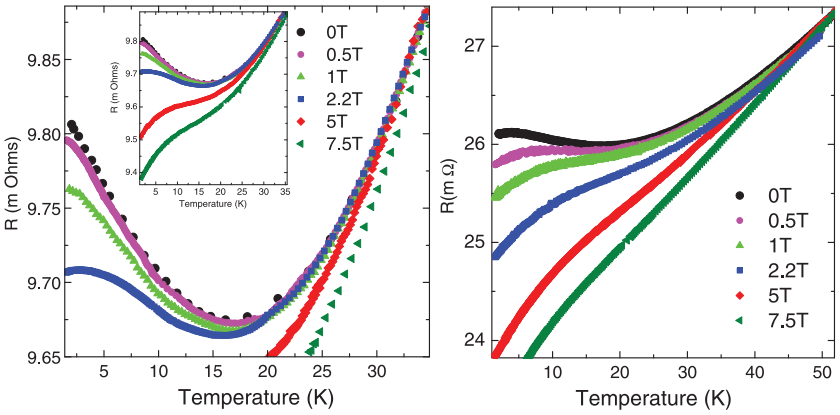

FIG. 11. (Color online) Electrical resistivity with applied magnetic fields up to $7T$. Left: iron silver sample with 0.4% Fe prepared at 85 K, and (right) iron silver sample with 0.3% Fe prepared at 285 K.

0.5, and 0.8% Fe and its minimum for 1.0, 1.2, and 1.5%. The change from a regime with a distinct resistivity minimum to a smeared-out regime is attributed to inhomogeneities of the system. The straight line in Fig. 2 indicates 4.2 K. The spectra taken at this temperature are shown on the right side of Fig. 2. It illustrates why the spectra for Fe $< 1.0\%$ reveal no static magnetic hyperfine interaction at this temperature, since the freezing is very close to 4.2 K. For the higher concentrations, T_{on} are again in fair agreement with the observed onset of the magnetic hyperfine interaction from the Mössbauer data.

A similar case where single substitutional iron impurities up to a range of concentrations of about 1.5% give rise to the Kondo effect has been reported for the system Zn:Fe (see Ref. 25). Also, Zn has negligible solubility for iron. In contrast to Ag:Fe, only monomers and no clusters of iron could be traced from the Mössbauer spectra. The breakdown of the Kondo effect due to magnetic interactions only occurs for concentrations above 2% Fe.

From the inspection of Figs. 3 and 10, the disappearance of the Kondo minimum in Ag:Fe seemingly occurs in parallel to the vanishing of the monomer and also of the clusters of type $D1$ contributions in the Mössbauer spectra. There is no clear indication for Kondo scattering when clusters of type $D11$ become dominant. From Figs. 8 and 9, however, we can see

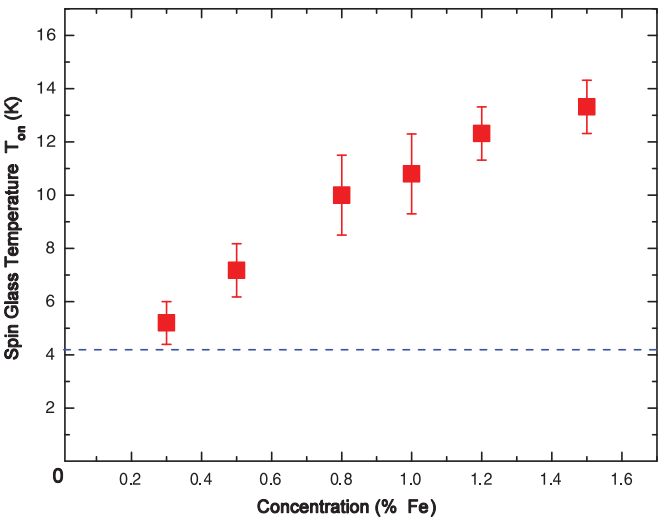

FIG. 12. (Color online) Onset temperature T_{on} for spin freezing, derived from resistivity data, for samples prepared at 285 K.

that even in the presence of large fractions of monomers and clusters of type $D1$, the Kondo effect may be suppressed. To derive a consistent picture of the concentration dependence of the Kondo effect in this system, we still need further systematic data.

From the disappearance of the resistance minimum with increasing Fe concentration, we can, however, exclude that the Kondo-like dependence of resistance is caused by weak localization, since this should become more apparent with increasing disorder, i.e., for the higher concentrations.

IV. CONCLUSIONS

In summary we have observed, from Mössbauer spectroscopy, the formation of two kinds of nanosized iron clusters in silver films prepared by codeposition from iron and silver atomic beams, under various preparation conditions and for several concentrations. The clusters occur in addition to monomeric iron and possess distinct hyperfine parameters. Samples containing a low amount of clusters reveal a resistivity minimum typical for the Kondo effect; those containing a high amount of clusters show a nonmonotonic resistivity behavior expected for spin-glass freezing competing with the Kondo effect. Spin-glass freezing is also clearly visible from the appearance of magnetic hyperfine splitting, and from magnetization and susceptibility data. The found spin-glass transition temperatures are in good agreement with estimates from a RKKY model for interacting clusters. The Mössbauer spectra in an applied magnetic field and magnetization data indicate cluster moments on the order of 40 μ_B, i.e., the clusters comprise only a few atoms.

Further support for a spin-glass transition and cluster moments of comparable magnitude comes from very recent low-energy muon spin rotation experiments performed at the Paul Scherrer Institute, Switzerland. Moreover, our first extended x-ray–absorption fine structure (EXAFS) studies are also compatible with extremely small cluster sizes.

ACKNOWLEDGMENTS

This work has been made possible by financial support from FAPERJ, CNPq/DFG, CAPES, and DAAD. Many helpful discussions with Hans Micklitz are gratefully acknowledged. W.T.H. and S.M.R. acknowledge financial support from CLAF/CNPq and PNPD/CNPq, respectively.

*william@cbpf.br

[1]M. A. Morales, E. C. Passamani, and E. Baggio-Saitovitch, Phys. Rev. B **66**, 144422 (2002).
[2]C. Larica, E. M. Baggio-Saitovitch, S. K. Xia, J. Magn. Magn. Mater. **110**, 106 (1992).
[3]C. Peng, S. Zhang, G. Li, and D. Dai, J. Appl. Phys. **76**, 998 (1994).
[4]J. A. Gómez, S. K. Xia, E. C. Passamani, B. Giordanengo, and E. M. Baggio-Saitovitch, J. Magn. Magn. Mater. **223**, 112 (2001).
[5]G. Longworth and R. Jain, J. Phys. F **8**, 993 (1978).
[6]G. Marest, H. Jaffrezic, J. Stanek, and H. Bineczycka, Nucl. Instrum. Methods **80-81**, 357 (1993).
[7]P. Steiner and S. Hüfner, Phys. Rev. B **12**, 842 (1975).
[8]E. M. Baggio-Saitovitch, J. Terra, and J. F. Litterst, Phys. Rev. B **39**, 6403 (1989).
[9]N. Kataoka, K. Sumiyama, and Y. Nakamura, J. Phys. F **18**, 1049 (1988).
[10]M. M. Pereira de Azevedo *et al.*, J. Magn. Magn. Mater. **173**, 230 (1997).
[11]G. Rollmann, P. Entel, and S. Sahoo, Comput. Mater. Sci. **35**, 275 (2006).
[12]P. J. Cregg and L. Bessais, J. Magn. Magn. Mater. **202**, 554 (1999).
[13]D. Altbir, J. d'Albuquerque e Castro, and P. Vargas, Phys. Rev. B **54**, R6823 (1996).
[14]D. Riegel, L. Büermann, K. D. Gross, M. Luszik-Bhadra, and S. N. Mishra, Phys. Rev. Lett. **61**, 2129 (1988).
[15]D. Riegel, L. Büermann, K. D. Gross, M. Luszik-Bhadra, and S. N. Mishra, Phys. Rev. Lett. **62**, 316 (1989).
[16]M. Hanson, J. Phys. F **7**, 2555 (1977).
[17]S. N. Mishra, P. Taneja, P. Ayyub, and A. A. Tulapurkar, Physica B **312-313**, 162 (2002).
[18]A. Crépieux and C. Lacroix, Physica B **259-261**, 204 (1999).
[19]A. Crépieux and C. Lacroix, Phys. Rev. B **59**, 13824 (1999).
[20]J. F. DiTusa, K. Lin, M. Park, M. S. Isaacson, and J. M. Parpia, Phys. Rev. Lett. **68**, 678 (1992).
[21]Guanlong Chen and N. Giordano, Phys. Rev. Lett. **66**, 209 (1991).
[22]U. Larsen, Phys. Rev. B **14**, 4356 (1976).
[23]M. G. Vavilov, L. I. Glazman, and A. I. Larkin, Phys. Rev. B **68**, 075119 (2003).
[24]J. S. Schilling, P. J. Ford, U. Larsen, and J. A. Mydosh, Phys. Rev. B **14**, 4368 (1976).
[25]P. Munayco, J. Larrea J., Y. T. Xing, H. Micklitz, and E. M. Baggio-Saitovitch, Phys. Rev. B **74**, 014423 (2006).